Optics and nonlinear effects in repetitive systems

Martin Berz *, Kyoko Makino

Department of Physics and Astronomy, Michigan State University, East Lansing, MI 48824-2320, USA

ARTICLE INFO

ABSTRACT

The weakly nonlinear dynamics in repetitive systems like synchrotrons, storage rings, linacs, and many new compact accelerators in the class of FFAGs is determined by criteria different from those in single pass optical systems. In the latter case, a clean description is obtained by the aberrations, i.e. nonlinear terms in the Taylor representation of the transfer map, and possible connections between them because of the symplectic symmetry of Hamiltonian systems or geometric symmetries of the system under consideration. For repetitive systems other criteria are relevant because conventional aberrations can be either enhanced or weakened by the repeated passage through the same system.

We begin with methods that provide highly accurate representations of fields, a pre-requisite for a detailed analysis of nonlinear motion, and discuss surface-based methods that assure accurate field representation far from midplane or axis. We then discuss methods to enforce the symplectic symmetry of the motion by minimal deformations in a suitable metric of Hamiltonian spaces, which is important in the attempt of long-term tracking of the dynamics. We then develop an analytical mechanism most closely related to the conventional aberration correction in conventional systems, the method of normal forms. As a result, quantitative measures of those linearities that matter are obtained in the form of resonance strengths and tune shifts. Residual effects can be described quantitatively using normal form defect methods, which allow rigorous predictions of long-term stability.

For practical calculations, the above methods can be expressed seamlessly in terms of differential algebraic structures on Taylor representations, either in a truncated representation in the conventional DA framework, or under consideration of remainder error terms in a fully rigorous setting.

© 2011 Elsevier B.V. All rights reserved.

1. Introduction

Particle optical systems are frequently described in terms of the transfer map $\mathcal{M}$, which represents the flow of the system ODE, as

$$\vec{z}_f = \mathcal{M}(\vec{z}_i, \vec{\delta})$$

where $\vec{z}_i$ and $\vec{z}_f$ are the initial and the final condition, $\vec{\delta}$ is system parameters. It is well known that the linear parts of the transfer map describe basic properties like magnifications, imaging conditions, while nonlinear parts describe various types of aberrations. For the use in conventional imaging and transport devices, the use of the transfer matrix in a Taylor representation is particularly useful since individual coefficients represent particular aberrations that have to be corrected, and the fact that certain system nonlinearities produce only certain aberrations simplifies the procedure.

For repetitive systems, the main interest of this paper, the individual nonlinearities of the map are not of primary interest,

but there are other descriptive quantities that can be derived from it, as will be discussed in Section 3. However, the transfer map holds the distinct advantage that it contains the entire information about the system, up to the accuracy to which it is determined, and it is not necessary to integrate orbits repeatedly in any way. This can result in significant speed advantages compared to conventional integration methods.

The practical computation of maps has been significantly simplified by the use of DA methods [1,2], and in simpler cases, the TPSA approach [3]. The method works to arbitrary order, allow to include system parameters, and lead to very efficient algorithms with an implementation effort independent of the computation order, thus significantly going beyond earlier approaches that are limited to customary third [4–7] or fifth order [8]. Since its introduction, the method has been widely utilized in a large number of new map codes [9–16].

The basic idea behind the method is to bring the treatment of functions to the computer in a similar way as the treatment of numbers, and that it is arithmetically possible to extract more information about a function than its mere values. Indeed, one defines the operation T to be the extraction of the Taylor coefficients of a pre-specified order n of the function. In mathematical terms, T is an equivalence relation, and the application of

* Corresponding author.
E-mail address: berz@msu.edu (M. Berz).

T corresponds to the transition from the function to the equivalence class comprising all those functions with identical Taylor expansion to order n. Since Taylor coefficients of order n for sums and products of functions as well as scalar products with reals can be computed from those of the summands and factors, it is clear that the diagram can be made to commute; indeed, except for the underlying inaccuracy of the floating point arithmetic, it will even commute exactly. In mathematical terms, this means that the set of equivalence classes of functions can be endowed with well-defined operations, leading to the so-called Truncated Power Series Algebra (TPSA) [17,3].

This fact was realized in the first paper on the subject [3], which led to a method to extract maps to any desired order from a computer algorithm that integrates orbits numerically. Similar to the need for algorithms within floating point arithmetic, the development of algorithms for functions followed, including methods to perform composition of functions, to invert them, to solve nonlinear systems explicitly, and to introduce the treatment of common elementary functions [18,19]. Very soon afterward it became apparent [1,20] that this only represents a half-way point, and one should proceed beyond mere arithmetic operations on function spaces of addition and multiplication and consider their analytic operations of differentiation and integration. This resulted in the recognition of the underlying differential algebraic structure and its practical exploitation [2], based on the commuting diagrams for addition, multiplication, and differentiation and their inverses:

$$
\begin{array}{ccccccc}
f,g & \xrightarrow{\;T\;} & F,G & \quad & f & \xrightarrow{\;T\;} & F \\[4pt]
{\scriptstyle +,-,\cdot,/}\Big\downarrow\;\;\Big\downarrow & & \oplus,\ominus,\odot,\oslash & \quad & \partial,\partial^{-1}\Big\downarrow\;\;\Big\downarrow & & \partial_{\bigcirc},\partial_{\bigcirc}^{-1} \\[4pt]
f_{-}^{+}g, f_{/}g & \xrightarrow{\;T\;} & F\overset{\oplus}{\underset{\ominus}{}}G, F\overset{\odot}{\underset{\oslash}{}}G & \quad & \partial f, \partial^{-1}f & \xrightarrow{\;T\;} & \partial_{\bigcirc}F, \partial_{\bigcirc}^{-1}F
\end{array}
\tag{1}
$$

In passing we note that in order to avoid loss of order, in practice the derivations have the form $\partial = h \cdot d/dx_i$, where h is a function with $h(0)=0$. As a first consequence, it allowed to construct integration techniques to any order that for a given accuracy demand are substantially faster and more general than conventional methods [19]. Subsequently, it was realized that the differential algebraic operations are useful for a whole variety of other questions connected to the analytic properties of the transfer map [18]. It was possible to determine arbitrary order generating function representations of maps [19,21]; factorizations into Lie operators [22] could be carried out for the first time to arbitrary order [19]; normal form methods [23,24] could be performed to arbitrary order [19,25]. And last but not least, the complicated PDEs for the fields and potentials stemming from the representation of Maxwell's equations in particle optical coordinates could be solved to any order in finitely many steps [2]. Finally, it is possible to extend the treatment to not only include Taylor coefficients, but also rigorous treatment of the error terms in the Taylor expansion, which leads to the concept of Taylor models [26–28].

2. High-order representation of fields

2.1. Description from midplane data

In many subfields of particle optics, the fields and potentials describing the motion of the particles are described in terms of their values in the midplane, as in the case of existing midplane symmetry, and in terms of their values on the reference axis, as in the case of discrete or continuous rotational symmetry.

In the case of round lenses used in electron microscopy and related fields, a long list of field models capturing the dominating

effects based on a few parameters exist; see for example [29]. For the case of spectrographs, storage rings and other devices based on fields with midplane symmetry, the approach usually consists of patching together regions in which the leading field multipoles do not depend on the position along the axis, and the so-called fringe-field region, where these leading field terms gradually fall-off from their value inside the element to zero. One frequently and successfully used model is the so-called Enge fall-off, given by modulating the main field values by the function:

$$
F(s) = \frac{1}{1 + \exp(a_1 + a_2 \cdot (s/D) + \cdots + a_6 \cdot (s/D)^5)}
\tag{2}
$$

where s is the position along the reference orbit, D is the aperture of the element, and usually the coefficients are normalized, so that the integral from far outside to far inside equals that of a step function with step at the effective field boundary.

High-order out-of-plane expansions can be done via recursion formulas (see Refs. [2,4,30,31] and references therein) and require the higher derivatives of the field fall-off. One of the simplest applications of the DA method is to compute these derivatives accurately. To illustrate this feature, we show the field fall-off profile of the default model for magnetic quadrupoles in COSY INFINITY, and their derivatives up to order five in Fig. 1, and to show that the orders do not represent a limitation, orders 10, 20, and 30 in Fig. 2.

As mentioned, recursion formulas can be used to obtain Taylor coefficients for out-of-plane data; but it turns out that there is a much easier way. However, the DA mechanism affords a much more elegant and general approach by virtue of the anti-derivation operator ∂^{-1}, which allows to determine the DA representation of the entire potential to order n in n steps. Consider the rather general PDE

$$
a_1 \frac{\partial}{\partial x}\left(a_2 \frac{\partial}{\partial x}V\right) + b_1 \frac{\partial}{\partial y}\left(b_2 \frac{\partial}{\partial y}V\right) + c_1 \frac{\partial}{\partial z}\left(c_2 \frac{\partial}{\partial z}V\right) = 0
$$

where a_i, b_i, c_i are functions of x, y, z. The PDE is re-written in fixed point form as

$$
\begin{aligned}
V = V|_{y=0} &+ \int_0^y \frac{1}{b_2}\left(b_2 \frac{\partial V}{\partial y}\right)\Big|_{y=0} \\
&- \int_0^y \frac{1}{b_2}\int_0^y \left(\frac{a_1}{b_1}\frac{\partial}{\partial x}\left(a_2 \frac{\partial V}{\partial x}\right) + \frac{c_1}{b_1}\frac{\partial}{\partial z}\left(c_2 \frac{\partial V}{\partial z}\right)\right)dy\,dy.
\end{aligned}
$$

Assume the derivatives of V and $\partial V/\partial y$ with respect to x and z are known in the plane $y=0$; these are precisely the terms that are obtained from the field model of interest. Then the right-hand side represents a contracting operator [2] with respect to y (which is necessary for the DA fixed point theorem), and the various orders in y can be iteratively calculated by mere iteration.

2.2. Description from surface data

As discussed in the previous section, a frequently used practice is the approximation of the electric and magnetic fields by models for the midplane, and then utilizing out-of-plane expansion for the subsequent steps. However, this method relies on the convergence of the resulting Taylor expansion to the true solution, which is a priori not guaranteed. One method to remedy the situation is to require during the fitting of model coefficients as in Eq. (2) that not only that the field is accurately described in the midplane, but also rather that the resulting out-of-plane expansion represent known measured or calculated data sufficiently away from the midplane. However, aside from the fact that this often makes the fitting procedure significantly more cumbersome, it often
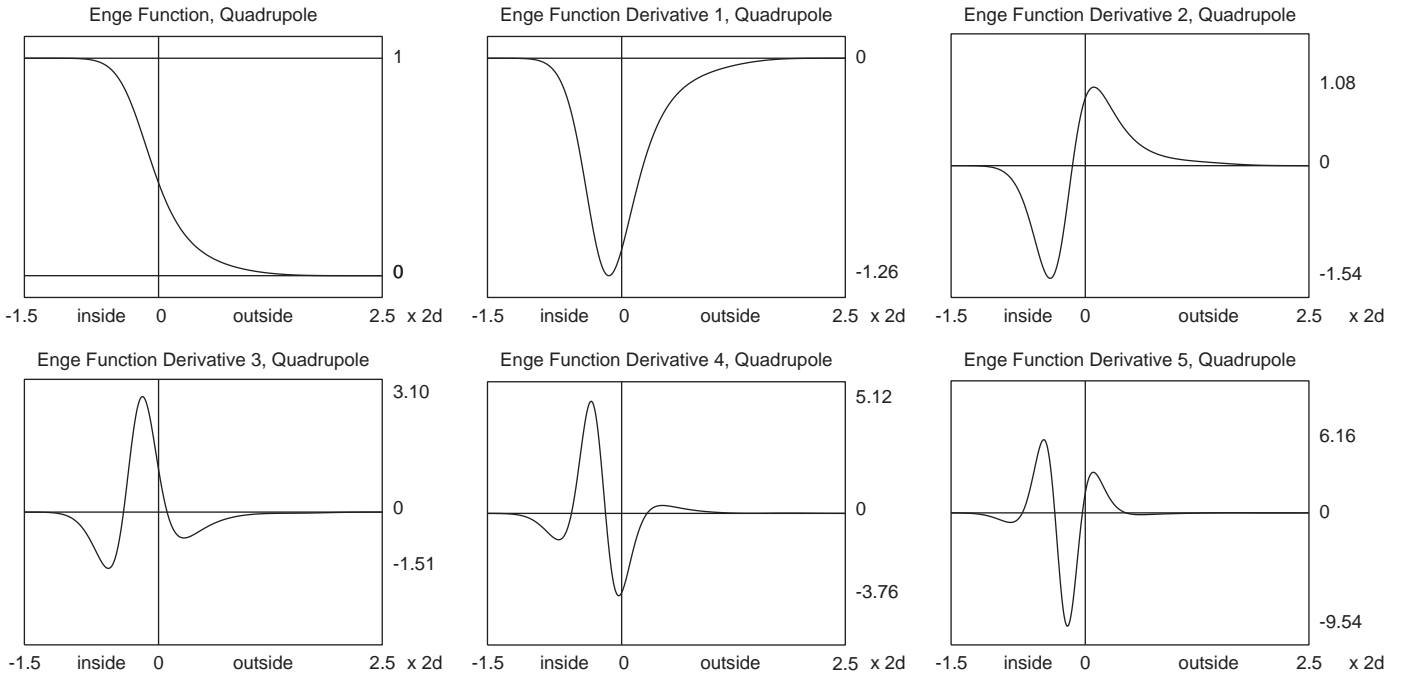
Fig. 1. Fringe field fall-off profile of the COSY default model for magnetic quadrupoles, and derivatives 1–5.
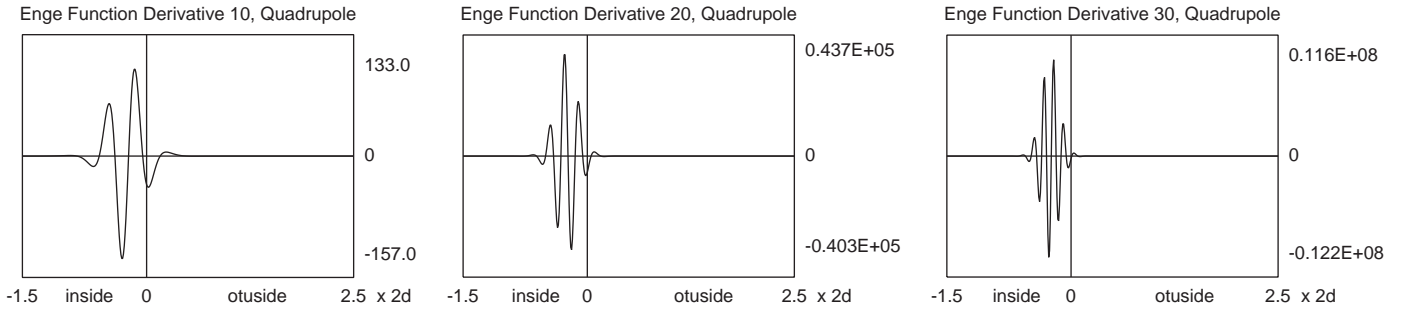
Fig. 2. Fringe field fall-off of the COSY default model for magnetic quadrupoles, derivatives 10, 20, and 30.

turns out that the desired result cannot be achieved or requires an impractical number of additional parameters.

However, there is an another approach that does not require any fitting, directly takes into account computed or measured field data suitably far from the midplane, and leads to converging out-of-midplane expansions. It is based on the Helmholtz theorem, which states that any vector field $\vec{B}$ that vanishes at infinity can be written as the sum of two terms, one of which is called "irrotational" and the other "solenoidal" as

$$\vec{B}(\vec{x}) = \vec{\nabla} \times \vec{A}_t(\vec{x}) + \vec{\nabla}\phi_n(\vec{x}) \text{ where}$$

$$\phi_n(\vec{x}) = \frac{1}{4\pi}\int_{\partial\Omega} \frac{\vec{n}(\vec{x}_s) \cdot \vec{B}(\vec{x}_s)}{|\vec{x}-\vec{x}_s|} ds - \frac{1}{4\pi}\int_{\Omega} \frac{\vec{\nabla} \cdot \vec{B}(\vec{x}_v)}{|\vec{x}-\vec{x}_v|} dV$$

$$\vec{A}_t(\vec{x}) = -\frac{1}{4\pi}\int_{\partial\Omega} \frac{\vec{n}(\vec{x}_s) \times \vec{B}(\vec{x}_s)}{|\vec{x}-\vec{x}_s|} ds + \frac{1}{4\pi}\int_{\Omega} \frac{\vec{\nabla} \times \vec{B}(\vec{x}_v)}{|\vec{x}-\vec{x}_v|} dV \quad (3)$$

where Ω is a connected region of interest, $\partial\Omega$ its boundary, is a surface which bounds the volume Ω, $\vec{x}_s$ and $\vec{x}_v$ denote points on $\partial\Omega$ and within Ω, $\vec{\nabla}$ denotes the gradient with respect to $\vec{x}_v$, and $\vec{n}$ is a unit normal vector pointing away from $\partial\Omega$. In the specific case, where $\vec{B}$ is the magnetic or electric field in the source free

region, we have $\vec{\nabla} \times \vec{B}(\vec{x}_v) = 0$ and $\vec{\nabla} \cdot \vec{B}(\vec{x}_v) = 0$, and the volume integral terms vanish, and so $\phi_n(\vec{x})$ and $\vec{A}_t(\vec{x})$ are completely determined from the normal and the tangential field data on surface $\partial\Omega$ via

$$\phi_n(\vec{x}) = \frac{1}{4\pi}\int_{\partial\Omega} \frac{\vec{n}(\vec{x}_s) \cdot \vec{B}(\vec{x}_s)}{|\vec{x}-\vec{x}_s|} ds$$

$$\vec{A}_t(\vec{x}) = -\frac{1}{4\pi}\int_{\partial\Omega} \frac{\vec{n}(\vec{x}_s) \times \vec{B}(\vec{x}_s)}{|\vec{x}-\vec{x}_s|} ds$$

$$\vec{B}(\vec{x}) = \vec{\nabla} \times \vec{A}_t(\vec{x}) + \vec{\nabla}\phi_n(\vec{x}). \quad (4)$$

The Helmholtz field representation has various advantages in addition to being able to find the field directly from the surface data. Specifically, the integral kernels that provide interior fields in terms of the boundary fields or source are smoothing, and most importantly, since the expressions in the kernel are analytic, they can be expanded at least locally. A detailed discussion of this approach can be found in Refs. [32–34] and references therein; it is particularly noteworthy that this method not only allows for converging representations, but also even allows a rigorous estimate of the error of the representation [35].
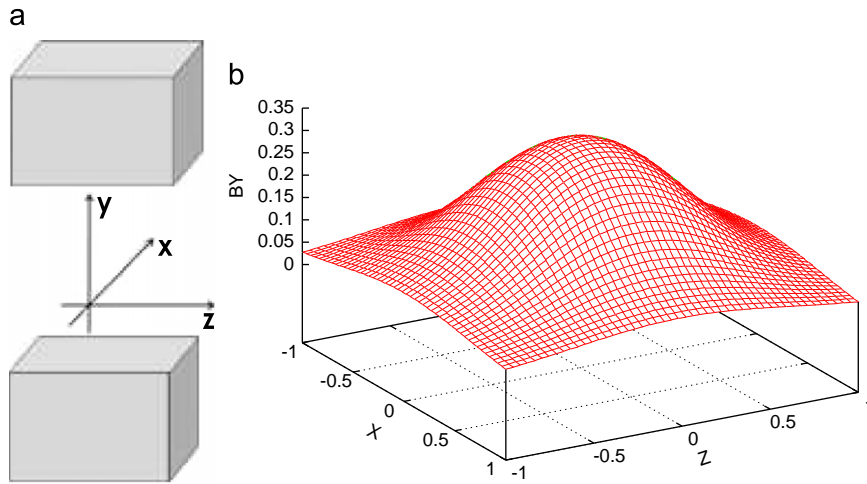
Fig. 3. Geometric layout of the bar magnet, consisting of two semi-infinite bars of magnetized material and the resulting magnetic field in the midplane.
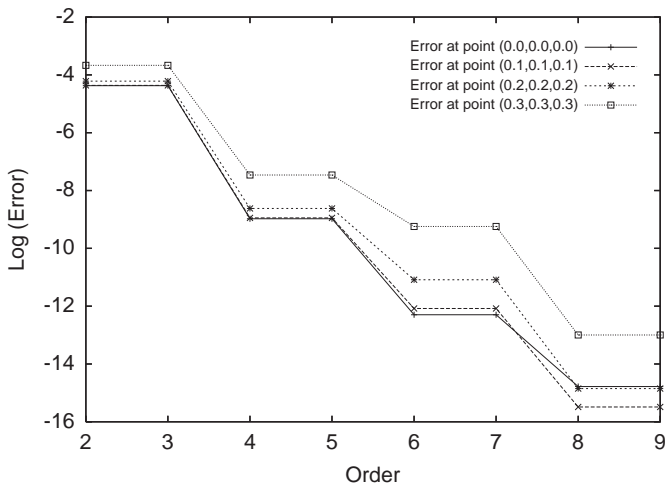
Fig. 4. Relative accuracy of the computation of the field using the Helmholtz expansion as a function of computation order.

To illustrate the performance of the method, we utilize an analytical model for which the field is known everywhere in space and which is frequently used as an example of a model for a dipole shown in Fig. 3. The field of this configuration in space is given by

$$B_y(x,y,z) = \frac{B_0}{4\pi} \sum_{i,j=1}^{2} (-1)^{i+j} \left[\arctan\left(\frac{X_i \cdot Z_j}{Y_+ \cdot R_{ij}^+}\right) + \arctan\left(\frac{X_i \cdot Z_j}{Y_- \cdot R_{ij}^-}\right) \right]$$

$$B_x(x,y,z) = \frac{B_0}{4\pi} \sum_{i,j=1}^{2} (-1)^{i+j} \left[\ln\left(\frac{Z_j + R_{ij}^-}{Z_j + R_{ij}^+}\right) \right]$$

$$B_z(x,y,z) = \frac{B_0}{4\pi} \sum_{i,j=1}^{2} (-1)^{i+j} \left[\ln\left(\frac{X_i + R_{ij}^-}{X_i + R_{ij}^+}\right) \right] \tag{5}$$

where $X_i = x - x_i$, $Y_\pm = y_0 \pm y$, $Z_i = z - z_i$, and $R_{ij}^\pm = (X_i^2 + Y_j^2 + Z_\pm^2)^{1/2}$. To assess and illustrate the performance of the method, the surface domain $\partial\Omega$ is chosen as a cube $-0.5 \le x \le 0.5$, $|y| \le 0.5$, and $-0.5 \le z \le 0.5$, and of which each face is split into a mere 44×44 mesh of subregions. On the reference plane, the field expansion is determined by evaluating the Helmholtz formula (4)

in DA arithmetic, and the resulting derivatives are re-used for an out-of-plane expansion. The resulting accuracy that can be obtained is shown in Fig. 4 for various points as a function of order; it is seen that despite the relatively modest surface integration mesh, for higher orders the resulting accuracy far exceeds other commonly used techniques. More details about the method can be found in Refs. [32,34].

3. Repetitive motion in complicated fields

As an example of the use of the field representations in the previous sections and the resulting challenges, we address the dynamics in a so-called FFAG [36,37]. This type of accelerator combines focusing and acceleration in a single device similar to case of a cyclotron, but while keeping tunes nearly constant throughout the acceleration region. Fig. 5 shows the resulting rather complicated midplane field of a one of six sectors of a contemplated FFAG in two different projections. We now assess the performance of such a device by repetitive tracking using the high-order transfer map of a particle of energy 1.1 MeV. We show the motion based on a third order transfer map (Fig. 6), as well as a transfer map of order 11 (Fig. 7) for motion in the $x-p_x$ and $y-p_y$ planes. It is apparent that there are very clear differences in the predicted stability of the orbits, in that the region of stability predicted increases by a factor of two or three for the x and y dynamics, respectively, when utilizing the higher orders.

However, even at these relatively high orders, the outer fringes of the motion exhibit some significant nonlinearity and spurious motion. This effect is due to the violation of an inherent symmetry of Hamiltonian systems, namely the symplecticity of the resulting transfer map [2,38,39]. There are a large number of methods to preserve the symplecticity of motion under repetitive tracking, one of the greatest challenges being to introduce as few correctional effects as possible. This matter is quite generally and successfully addressed by considering Hamiltonian motion in a suitable metric, which allows the development of a large class of symplectification methods [40–42] that preserve the symplecticity by performing only minimal correction to the dynamic, as opposed to various earlier methods [2,21,43]. In Fig. 8, we show the situation with symplectification based on the minimal correction symplectification approach. It is apparent that for both planes the region of stability increases, and furthermore, a rich structure of islands begins to appear in the $x-p_x$ motion.
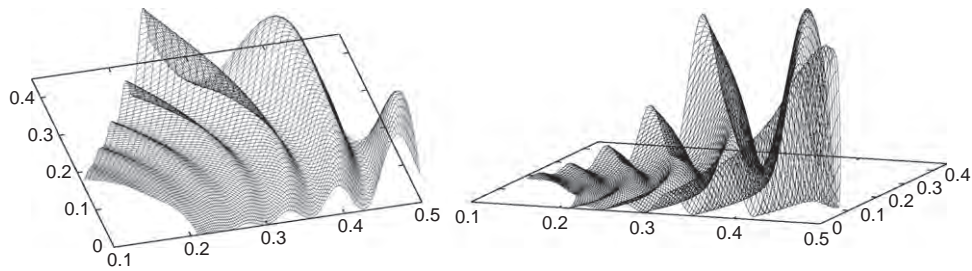
Fig. 5. B_y field profile, shown from different viewing angles. The 3D filed was obtained by the DA out-of-plane field expansion.
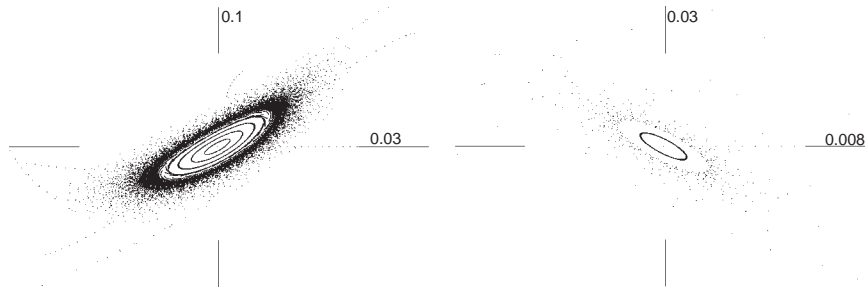
Fig. 6. FFAG dynamics, third order, no symplectification.
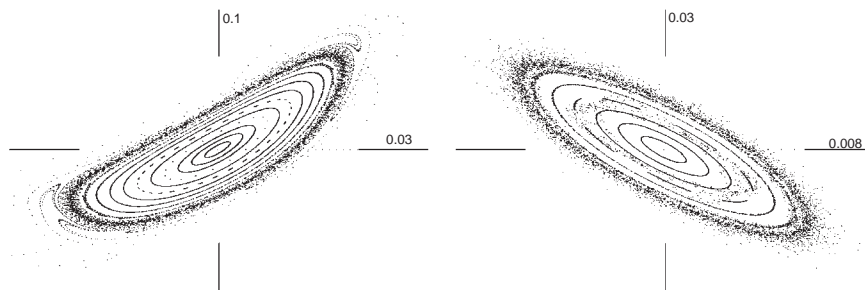
Fig. 7. FFAG dynamics, 11th order, no symplectification.
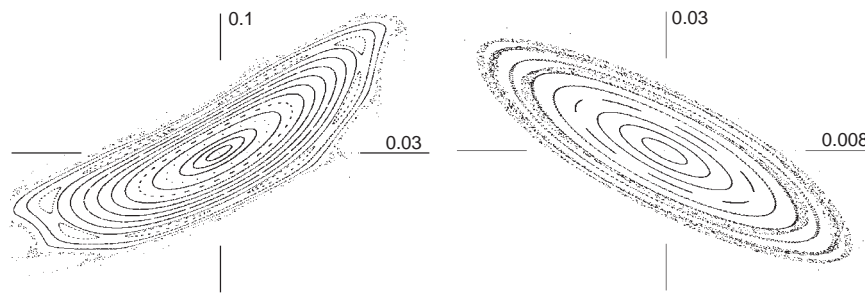
Fig. 8. FFAG dynamics, 11th order, with symplectification.

4. Normal form methods

When studying repetitive motion, the understanding of the consequence of nonlinear effects follows other necessities than in the case of single pass motion. In the latter, it is usually individual nonlinearities, or aberrations, that need to be understood and corrected, while in the former, individual aberrations are often unimportant because over sufficiently many turns, their effects average out. Indeed, the choice of tunes and the linear layout of accelerator lattices are often expressly chosen for this very purpose.

The natural way to study nonlinear motion in repetitive systems is through the use of a tool that filters aberrations into those that matter, and those are irrelevant. This is achieved by switching to coordinate systems that in a step-by-step manner lead to representations in which the transfer map is invariant under rotations R, i.e.

$$\mathcal{M} \circ \mathcal{R} = \mathcal{R} \circ \mathcal{M}. \tag{6}$$

In the map is symplectic, then this confines the motion to circles; if it is damped, we obtain logarithmic spirals. The great advantage of this approach is that if the motion is rotationally invariant and symplectic, there is no doubt about its long-term behavior—it is stable.

The effects of existing instabilities due to nonlinearities in the motion then manifest themselves in the amount to which the condition (6) is violated, the so-called invariant defect, i.e. the
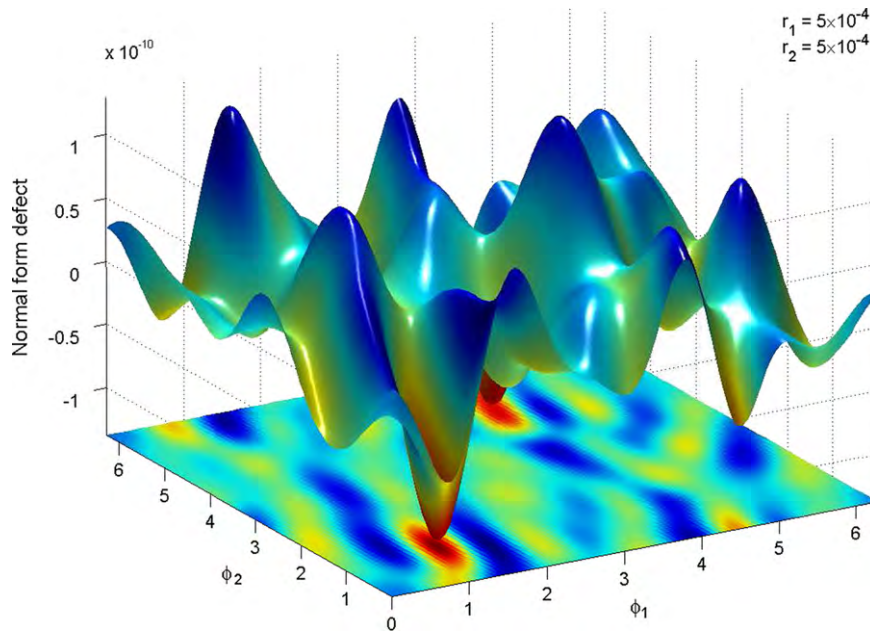
Fig. 9. A 2D projection of a normal form defect function. Note the very small scale of approximately 10^{-10}, showing the high quality of the normal form transformation. Picture courtesy Youn-Kyung Kim.

bound of $\mathcal{M} \circ \mathcal{R} - R \circ \mathcal{M}$. In fact, if there is any single equivalent for repetitive systems to the concept of aberrations in the case of single pass systems, it is this single measure of the aberration from rotationally invariant motion.

In addition, the normal form transformation has other advantages, in particular that other frequently needed quantities such as the dependence of tune on amplitude and the strengths of resonances are readily computable. At its core, the normal form method rests on iteratively subjecting the map to nonlinear transformations of the form $\mathcal{A}_m = \mathcal{E} + \mathcal{T}_m$ where $\mathcal{E}$ is the identity and $\mathcal{T}_m$ is a map of exact order m. Noting that up to order m, the inverse is $\mathcal{A}_m^{-1} = {}_m\mathcal{E} - \mathcal{T}_m$, we obtain for the correction of the map $\mathcal{R} + \mathcal{S}_{m-1}$ from the $(m-1)$st step:

$$\mathcal{A} \circ \mathcal{M} \circ \mathcal{A}^{-1} = {}_m(\mathcal{E} + \mathcal{T}_m) \circ (\mathcal{R} + \mathcal{S}_{m-1}) \circ (\mathcal{E} - \mathcal{T}_m)$$

$$= {}_m(\mathcal{E} + \mathcal{T}_m) \circ (\mathcal{R} + \mathcal{S}_{m-1}) \circ (\mathcal{E} - \mathcal{T}_m)$$
$$= {}_m \mathcal{R} + \mathcal{S}_{m-1} + (\mathcal{T}_m \circ \mathcal{R} - \mathcal{R} \circ \mathcal{T}_m).$$

Thus the commutator $\mathcal{T}_m \circ \mathcal{R} - \mathcal{R} \circ \mathcal{T}_m$ can be used for the correction by suitable choice of $\mathcal{T}_m$. This is not the place for further details, rather we refer the reader to Ref. [2].

Since the invariant defect is a direct measure of nonlinear effect detrimental to stability, it is very useful to determine bounds of it, and use it as a quantitative measure for the optimization of accelerator lattices. Furthermore, such bounds can then also be used for rigorous estimates of long-term stability as discussed in Refs. [27,44,45]. However, the invariant defect is the global maximum of a complicated function of six variables with a number of local maxima that increases with the quality of the stability, so its precise bound represents a significant challenge. To illustrate its complexity, in Fig. 9 we show part of a two-dimensional projection of the normal form defect function, exhibiting a large number of local minima and maxima over a very small range of function values. We used two rigorous global optimizers for this optimization task, the commonly used GlobSol [46] as well as the COSY-GO Optimizer [47].

The extreme difficulty and, in technical terms, strong cancellation problem present allowed COSY-GO with its strategies to avoid dependency to clearly outperform GlobSol by many orders of magnitude, as shown in Table 1.

Table 1
Results of global optimization of the normal form defect functions.

Dim	GlobSol		COSY-GO		
	CPU time (s)	# of boxes	CPU (s)	Max list	#boxes
2	18,810 s	4733	6	11	31
3	> 500,000 s	–	39	44	172
4	–	–	347	357	989
5	–	–	3971	2248	6641
6	–	–	57842	17241	49821

Acknowledgments

References

[1] M. Berz, Particle Accelerators 24 (1989) 109.
[2] M. Berz, Modern Map Methods in Particle Beam Physics, Academic Press, San Diego, 1999 Also available at ⟨http://bt.pa.msu.edu/pub⟩.
[3] M. Berz, Nuclear Instruments and Methods A 258 (1987) 431.
[4] K.L. Brown, The ion optical program TRANSPORT, Technical Report 91, SLAC, 1979.
[5] H. Wollnik, J. Brezina, M. Berz, Nuclear Instruments and Methods A 258 (1987) 408.
[6] T. Matsuo, H. Matsuda, Y. Fujita, H. Wollnik, Mass Spectrometry 24 (1976).
[7] A.J. Dragt, L.M. Healy, F. Neri, R. Ryne, IEEE Transactions on Nuclear Science NS-3,5 (1985) 2311.
[8] M. Berz, H.C. Hofmann, H. Wollnik, Nuclear Instruments and Methods A 258 (1987) 402.
[9] M. Berz, K. Makino, COSY INFINITY Version 8.1—user's guide and reference manual, Technical Report MSUHEP-20704, Department of Physics and Astronomy, Michigan State University, East Lansing, MI 48824, see also ⟨http://cosy.pa.msu.edu⟩, 2002.
[10] L. Michelotti, MXYZTPLK: a practical, user friendly C++ implementation of differential algebra, Technical Report, Fermilab, 1990.
[11] W. Davis, S.R. Douglas, G.D. Pusch, G.E. Lee-Whiting, The Chalk River differential algebra code DACYC and the role of differential and Lie algebras in understanding the orbit dynamics in cyclotrons, in: M. Berz, S. Martin, K. Ziegler (Eds.), Proceedings of the Workshop on Nonlinear Effects in Accelerators, IOP Publishing, London, 1993.

[12] J. van Zeijts, F. Neri, The arbitrary order design code TLIE 1.0, in: M. Berz, S. Martin, K. Ziegler (Eds.), Proceedings of the Workshop on Nonlinear Effects in Accelerators, IOP Publishing, London, 1993.

[13] J. van Zeijts, New features in the design code TLIE, in: Third Computational Accelerator Physics Conference, vol. 297, AIP Conference Proceedings, 1993, p. 285.

[14] Y. Yan, C.-Y. Yan, ZLIB, a numerical library for differential algebra, Technical Report 300, SSCL, 1990.

[15] Y. Yan, ZLIB and related programs for beam dynamics studies, in: Third Computational Accelerator Physics Conference, Vol. 297, AIP Conference Proceedings, 1993, p. 279.

[16] F.C. Iselin, The CLASSIC project, in: Fourth Computational Accelerator Physics Conference, vol. 297, AIP Conference Proceedings, 1997, p. 325.

[17] M. Berz, The new method of TPSA algebra for the description of beam dynamics to high orders, Technical Report AT-6:ATN-86-16, Los Alamos National Laboratory, 1986.

[18] M. Berz, Differential algebraic techniques, in: M. Tigner, A. Chao (Eds.), Handbook of Accelerator Physics and Engineering, World Scientific, New York, 1999.

[19] M. Berz, High-order computation and normal form analysis of repetitive systems, in: M. Month (Ed.), Physics of Particle Accelerators, vol. 249, American Institute of Physics, New York, 1991, p. 456.

[20] M. Berz, Differential algebraic description of beam dynamics to very high orders, Technical Report SSC-152, SSC Central Design Group, Berkeley, CA, 1988.

[21] M. Berz, Symplectic tracking in circular accelerators with high order maps, in: Nonlinear Problems in Future Particle Accelerators, World Scientific, 1991, p. 288.

[22] A.J. Dragt, J.M. Finn, Journal of Mathematical Physics 17 (1976) 2215.

[23] A.J. Dragt, J.M. Finn, Journal of Mathematical Physics 20 (12) (1979) 2649.

[24] A. Bazzani, Celestial Mechanics 42 (1988) 107.

[25] E. Forest, M. Berz, J. Irwin, Particle Accelerators 24 (1989) 91.

[26] K. Makino, M. Berz, Remainder differential algebras and their applications, in: M. Berz, C. Bischof, G. Corliss, A. Griewank (Eds.), Computational Differentiation: Techniques, Applications, and Tools, SIAM, Philadelphia, 1996, pp. 63–74.

[27] K. Makino, Rigorous analysis of nonlinear motion in particle accelerators, Ph.D. Thesis, Michigan State University, East Lansing, Michigan, USA, Also MSUCL-1093, 1998.

[28] M. Berz, AIP Conference Proceedings 405 (1997) 1.

[29] M. Berz, K. Makino, COSY INFINITY Version 9.0 beam physics manual, Technical Report, MSUHEP-060804, Department of Physics and Astronomy, Michigan State University, East Lansing, MI 48824, see also ⟨http://cosyinfinity.org⟩, 2007.

[30] K.L. Brown, R. Belbeoch, P. Bounin, Review of Scientific Instruments 35 (1964) 481.

[31] K.L. Brown, A first- and second-order matrix theory for the design of beam transport systems and charged particle spectrometers, Technical Report 75, SLAC, 1982.

[32] S.L. Manikonda, M. Berz, International Journal of Pure and Applied Mathematics 23 (3) (2005) 365.

[33] S.L. Manikonda, M. Berz, Nuclear Instruments and Methods 558 (1) (2006) 175.

[34] S. Manikonda, High order finite element methods to compute Taylor transfer maps, Ph.D. Thesis, Michigan State University, East Lansing, Michigan, USA, 2006.

[35] S.L. Manikonda, M. Berz, K. Makino, Transactions on Computers 4–11 (2005) 1604.

[36] C. Johnstone, S. Koscielniak, The new generation of FFAG accelerators, DPB Newsletter, American Physical Society, 2008, pp. 12–14.

[37] C. Johnstone, M. Berz, K. Makino, P. Snopok, Isochronous (CW) non-scaling FFAGs: design and simulation, in: Proceedings, 2010 Advanced Accelerator Concepts Workshop, in press, http://www.ireap.umd.edu/AAC2010/proceedings.htm.

[38] V.I. Arnold, S.P. Novikov (Eds.), Dynamical Systems IV, Symplectic Geometry and its Applications, Springer-Verlag, 1990.

[39] H. Wollnik, M. Berz, Nuclear Instruments and Methods 238 (1985) 127.

[40] B. Erdélyi, Symplectic approximation of Hamiltonian flows and accurate simulation of fringe field effects, Ph.D. Thesis, Michigan State University, East Lansing, Michigan, USA, 2001.

[41] B. Erdélyi, M. Berz, International Journal of Pure and Applied Mathematics 11 (3) (2004) 241.

[42] B. Erdélyi, M. Berz, Physical Review Letters 87 (11) (2001) 114302.

[43] J. Shi, Physical Review E 50 (1994) 1.

[44] M. Berz, K. Makino, Y.-K. Kim, Nuclear Instruments and Methods 558 (2006) 1.

[45] K. Makino, M. Berz, Y.-K. Kim, P. Snopok, Long term stability of large accelerators, ECMI Newsletter 39.

[46] R.B. Kearfott, Rigorous Global Search: Continuous Problems, Kluwer Academic Press, Dordrecht, 1996.

[47] K. Makino, M. Berz, Nucl. Instr. and Meth. A, in press, doi:10.1016/j.nima.2010.12.185.